Transport Properties of the Calcium Ionophore ETH-129

Exing Wang, Warren L. Erdahl, Shawn A. Hamidinia, Clifford J. Chapman, Richard W. Taylor,* and Douglas R. Pfeiffer

Department of Molecular and Cellular Biochemistry, The Ohio State University, Columbus, Ohio 43210 and *Department of Chemistry and Biochemistry, University of Oklahoma, Norman, Oklahoma 73019 USA

ABSTRACT The transport mechanism and specificities of ionophore ETH-29 have been investigated in a highly defined phospholipid vesicle system, with the goal of facilitating the application of this compound to biological problems. ETH-129 transports Ca^{2+} via an electrogenic mechanism, in contrast to A23187 and ionomycin, which function in a charge neutral manner. The rate of transport is a function of membrane potential, increasing by 3.9-fold per 59 mV over a broad range of that parameter. Rate is independent of the transmembrane pH gradient and strongly stimulated by the uncoupler carbonyl cyanide *m*-chlorophenylhydrazone when no external potential has been applied. The effect of uncoupler reflects the collapse of an opposing potential arising during Ca^{2+} transport, but also reflects the formation of a mixed complex between the uncoupler, ETH-129, and Ca^{2+} that readily permeates the vesicle membrane. Oleate does not substitute for the uncoupler in either regard. ETH-129 transports polyvalent cations according to the selectivity sequence $La^{3+} > Ca^{2+} > Zn^{2+} \approx Sr^{2+} > Co^{2+} \approx Ni^{2+} \approx Mn^{2+}$, with the magnitude of the selectivity coefficients reflecting the cation concentration range considered. There is little or no activity for the transport of Na^+, K^+, and Mg^{2+}. These properties suggest that ETH-129 will be useful for investigating the consequences of a mitochondrial Ca^{2+} overload in mammalian cells, which is difficult to pursue through the application of electroneutral ionophores.

INTRODUCTION

Ionophore ETH-129 (Fig. 1) belongs to a set of compounds synthesized by Simon and coworkers for use in the production of ion-selective electrodes (Pretsch et al., 1980). It is distinguished in that regard by allowing the construction of electrodes with subnanomolar sensitivity for Ca^{2+} and selectivities for that cation over Mg^{2+}, Na^+, and K^+ in the range of 10^5-10^8 (Schefer et al., 1986). Prestipino and coworkers demonstrated that ETH-129 transports Ca^{2+} across artificial phospholipid bilayer membranes and the limiting membranes of mitochondria and sea urchin eggs (Prestipino et al., 1993). We extended their results by demonstrating that the presence of ETH-129 allows yeast mitochondria to accumulate large amounts of Ca^{2+} even though they lack an endogenous activity (a Ca^{2+} uniporter) for the inward transport of that cation (Jung et al., 1997). Our results showed that ETH-129 is an efficient ionophore for Ca^{2+} in both isolated yeast mitochondria (Jung et al., 1997), and those that remain in intact cells (D. W. Jung, P. C. Bradshaw, M. Litsky, and D. R. Pfeiffer, submitted for publication). A related compound, ETH-1001, was introduced earlier by Simon and coworkers (Ammann et al., 1976) and shown to transport Ca^{2+} in similar systems (Caroni et al., 1977). However, in mitochondria, ETH-129 is more efficient than ETH-1001 by approximately 20-fold (Prestipino et al., 1993).

In a broader context, Ca^{2+} ionophores are used as general research tools in cell biology to manipulate intracellular Ca^{2+} concentrations and the signaling systems that are influenced by that parameter. Such studies normally use A23187, 4-BrA23187, or Ionomycin, which are carboxylic acid ionophores that transport Ca^{2+} by mechanisms that are strictly electroneutral (Erdahl et al., 1994, 1995; Thomas et al., 1997; Prabhananda and Kombrabail, 1998). That is to say, the transporting species do not carry a net charge, and Ca^{2+} is exchanged for $2H^+$, or other cations, such that no net charge movements accompany transport catalyzed by these compounds (Dobler, 1981; Westley, 1982). ETH-129 contains no ionizable functions and so forms cation complexes that do carry a charge, which is positive. Ionophores of this type are referred to as electrogenic, meaning that transmembrane charge movement does occur during transport catalyzed by members of this class (Dobler, 1981; Westley, 1982). Transport catalyzed by electroneutral ionophores is influenced by transmembrane pH gradients,

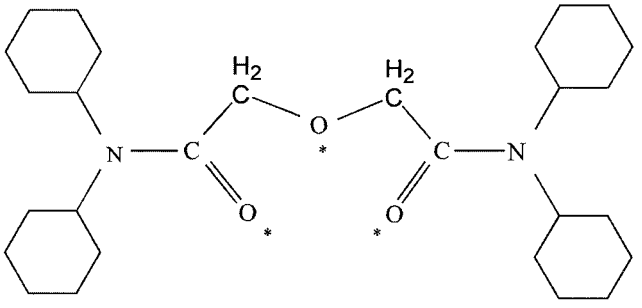

FIGURE 1 The bond-line structure of ionophore ETH-129. Ligand donor atoms (Ca^{2+} complex) are marked with an asterisk.

Received for publication 16 May 2001 and in final form 17 August 2001.

Address reprint requests to Douglas R. Pfeiffer, Ph.D., Dept. of Molecular and Cellular Biochemistry, The Ohio State University, 1645 Neil Ave., 310A Hamilton Hall, Columbus, OH 43210-1218. Tel.: 614-292-8774; Fax: 614-292-4118; E-mail: pfeiffer.17@osu.edu.

0006-3495/01/12/3275/10 $2.00

whereas membrane potential is important in the case of electrogenic ionophores (Woolley et al., 1995). This distinction could be exploited when investigating the biological roles of Ca^{2+} and Ca^{2+}-mediated processes. However, ETH-129 has not been used in such a fashion. This may reflect our modest understanding of the compound in terms of its transport properties and specificities, which makes it difficult to predict its potential behaviors under in vivo conditions. The present report expands upon the limited information available about ETH-129 and will thereby facilitate its application as a tool for basic research.

MATERIALS AND METHODS

Preparation of phospholipid vesicles

Unilamellar vesicles loaded with Quin-2 were prepared from 1-palmitoyl-2-oleoyl-*sn*-glycerophosphatidylcholine (POPC) by freeze–thaw extrusion (Erdahl et al., 1994, 1995). The formation medium contained 5 mM Quin-2 (K^+), 10 mM *N*-(2-hydroxyethyl)piperazine-*N*′-(2-ethanesulfonic acid (Hepes) (K^+), pH = 7.00, and 100 mM KCl. A high internal K^+ concentration was sought to allow the generation of membrane potentials of varying magnitude (see below). The preparations obtained were applied to Sephadex G-50 mini-columns and eluted by low speed centrifugation (Fry et al., 1978), to replace the external medium with a 10-mM Hepes buffer (Na^+), pH = 7.00 (Erdahl et al., 1994, 1995).

The nominal concentration of POPC in final preparations was determined as lipid phosphorus (Bartlett, 1959) and was near 80 mM. The average diameter of these vesicles is 71 nm as determined by freeze-fracture electron microscopy (Chapman et al., 1990). They contained entrapped K^+ at ~125 mM, as determined by atomic absorption spectroscopy, and Quin-2 at ~6 mM. The latter value was determined by titrating lysed vesicles with a standard solution of $CaCl_2$ and is about ⅓ of the value that we normally obtain (Erdahl et al., 1995). The reduced efficiency of Quin-2 entrapment is a consequence of the high solute level that was used in the vesicle formation medium during this study. High levels reduce the effectiveness of a freeze—thaw-driven solute-concentrating mechanism that normally elevates the internal concentrations of solutes relative to the external volume (Chapman et al., 1990, 1991).

The determination of cation transport

POPC vesicles containing Quin-2 were used at a nominal phospholipid concentration of 1.0 mM, and at 25°C. The external medium contained polyvalent cation salts as described in the figure legends, 100 mM NaCl, or mixtures of NaCl and KCl totaling 200 mM, and 10 mM Hepes, pH 7.00, unless otherwise noted. The medium pH was adjusted with NaOH that had been passed over Chelex 100 columns to remove contaminating cations (Erdahl et al., 1994).

In most cases, an inside negative membrane electrical potential was present during the experiments. This was generated by the presence of 0.5 μM valinomycin (Val), which transports K^+ out of the vesicles electrogenically (Erdahl et al., 1994). The magnitude of the potential was controlled by varying the concentration ratio of Na^+ to K^+ in the external medium. A tetraphenylphosphonium cation (TPP^+) electrode was used to measure the potential (Broekemeier et al., 1998), and thereby to verify that the calculated values were obtained. For these purposes the incubation medium contained 2.0 μM TPP·Cl, and the entrapped volume was taken to be 2.02 μl/ml at a nominal POPC concentration of 1.0 mM (Chapman et al., 1990). Electrode calibration experiments conducted in the presence and absence of vesicles, and of ETH-129, showed that binding of the probe to POPC was not significant and that the ionophore does not perturb the electrode, respectively. In the several preparations used, the observed potential showed a near-Nernstian relationship to variations in the transmembrane K^+ gradient (observed values changed by 56–60 mV per 10-fold change in the gradient). Val was omitted when an imposed membrane potential was not desired, or, in some cases, 5 μM of the protonophore carbonyl cyanide *m*-chlorophenylhydrazone (CCCP) was present instead of Val. The former condition allows formation of a membrane potential due to the action of ETH-129, whereas the latter condition does not.

The transport of polyvalent cations was monitored by difference absorbance measurements, which detect formation of the Quin-2:cation complex within the vesicle lumen. An Aminco DW2a spectrophotometer operating in the dual wavelength mode was used. In addition, an Oriel No. 59800 band pass filter was used between the cuvette and the beam scrambler-photomultiplier assembly to prevent detection of the fluorescent light emitted by Quin-2. The sample wavelength for all cations was 264 nm. The reference wavelengths were at an isosbestic point in the Quin-2/Quin-2:cation complex difference spectrum of interest. These wavelengths vary slightly from cation to cation, as previously described (Erdahl et al., 1996). Data were collected on disk using Unkel Scope software (Unkel Software, Inc., Lexington, MA) or the software system from On Line Instruments Systems Inc. (Bogart, GA), which accompanies their modification package for Aminco DW2 series spectrophotometers.

Other methods

Procedures used to obtain initial rates from the progress curves have been described previously (Erdahl et al., 1994). The *y* axis unit in figures containing these curves (Cation Accumulated, μM) refers to the external cation concentration, which decreases as the cation is transported into the vesicle lumen. Stock solutions of all ionophores were prepared in ethanol.

RESULTS

Effect of membrane potential on transport

To confirm the electrogenic nature of Ca^{2+} transport mediated by ETH-129, effects of membrane potential on the rate of transport were examined. Calcium ion permeates the limiting membrane of K^+ loaded POPC vesicles very slowly, and the presence of ETH-129 alone has only a modest effect on the rate of that process (Fig. 2 *A*; Erdahl et al., 1994, 2000). The latter observation is expected for an ionophore that acts by an electrogenic mechanism because a large inside positive membrane potential would arise quickly and oppose further activity. No potential is seen under these conditions (Fig. 2 *A*), however, it would not be observed by the TPP^+ electrode technique because of the inside positive orientation.

If the modest Ca^{2+} transport activity seen in Fig. 2 *A* were a consequence of an opposing potential, the presence of Val or CCCP would be expected to collapse it and allow transport to proceed more rapidly. Either agent has that effect, as shown in Fig. 2, *B* and *C*. In the case of Val, a large inside negative potential would be expected initially, due to the large K^+ concentration gradient, and this potential would be expected to decrease as Ca^{2+} transport proceeded. The latter result is anticipated because the net reaction when both ETH-129 and Val are present would be an exchange of Ca^{2+} (external) for $2K^+$ (internal). The K^+

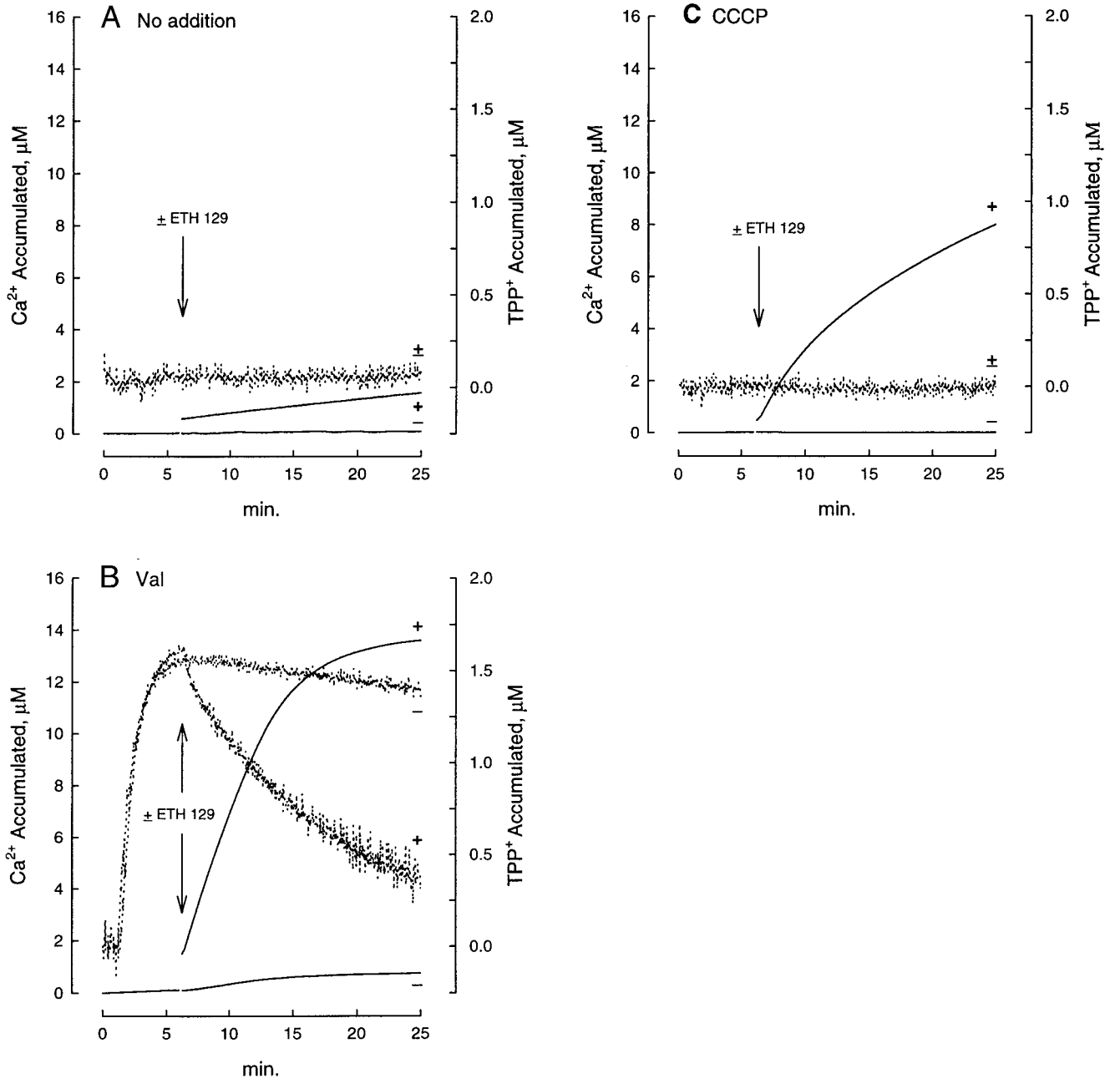

FIGURE 2 Conditions effecting ETH-129-mediated Ca^{2+} transport. POPC vesicles loaded with Quin-2 and K^+ were incubated in the NaCl-Hepes medium, as described in Materials and Methods. Techniques for monitoring Ca^{2+} accumulation (*solid lines*) and TPP^+ accumulation (*dotted lines*) were also as described in Materials and Methods. The nominal concentrations of POPC and Quin-2 were 1.0 mM and 14.2 μM, respectively. For all panels, 100 μM $CaCl_2$ and 2.0 μM TPP·Cl were present. 5.0 μM ETH-129 was added where indicated to initiate Ca^{2+} accumulation. (*A*) No further additions. (*B*) and (*C*) 0.5 μM Val or 5.0 μM CCCP was present from the beginning of the incubations, respectively. TPP^+ accumulation reflects formation of a membrane electrical potential that is oriented inside negative. Under the conditions used, accumulation of 1.5 μM TPP^+ corresponds to a potential of 187 mV.

concentration gradient would then decline progressively as Ca^{2+} transport proceeded, giving rise to the decreasing potential. Both of these expectations are as observed (Fig. 2 *B*). In the case of CCCP, which catalyzes an electrogenic transport of H^+, no potential is expected initially or as transport proceeds, and this is also as observed (Fig. 2 *C*).

Although the acceleration of Ca^{2+} transport produced by either Val or CCCP is consistent with ETH-129 acting through an electrogenic mechanism, the rate is clearly slower when the opposing potential is collapsed with CCCP instead of Val (compare Fig. 2, *B* and *C*). This difference is not expected a priori. It could indicate that the inside neg-

ative potential produced by Val, but not by CCCP, favors transport directly and not simply by collapsing an opposing potential. In contrast, a transmembrane pH gradient will form as Ca^{2+} transport proceeds in the presence of CCCP because the cation is then exchanged for H^+. This might influence the rate of transport by altering the protonation state of the ionophore or its Ca^{2+} complex, or the distribution of ETH-129 among multiple complexes with Ca^{2+}, if some are ternary complexes that involve OH^-. In addition, ternary complexes involving Ca^{2+}, ETH-129, and CCCP might arise and alter the rate of transport relative to that seen in the presence of Val.

To examine these various possibilities, we first varied the magnitude of the potential induced by Val and determined the effect on Ca^{2+} transport (Fig. 3). A linear relationship is seen between log of the transport rate and $\Delta\Psi$, with a slope value of 0.12 mV^{-1} and a rate at zero potential (extrapolated) of 0.41 nM/s. The slope value is equivalent to a 3.9-fold acceleration per 59 mV increase in $\Delta\Psi$, whereas the rate at zero potential, determined by extrapolation, is slightly lower than the rate seen when CCCP is used to eliminate an opposing potential (0.88 nM/s in Fig. 2 *C*). From these data, it is clear that membrane potential facilitates transport directly and that this contributes to the rate enhancement produced by Val that was shown in Fig. 2.

To further clarify the action of CCCP, effects of pH conditions were examined in the presence of a high potential. It first appears that the Ca^{2+} transport rate decreases as the external pH rises from 6.0 to 7.6, but is not changed in response to a further increase to pH = 8.2 (Fig. 4 *A*). However, when ETH-129 and Ca^{2+} are absent, the difference absorbance of entrapped Quin-2 shows time- and potential-dependent changes that are the same as those reflecting Ca^{2+} transport, and that have the same dependence on pH (Fig. 4 *B*). We interpret the latter data to indicate that uncatalyzed H^+ diffusion into the vesicles occurs when membrane potential is high, and that this is favored by acidic pH. As a result, the internal volume becomes progressively more acidic, the protonation state of entrapped Quin-2 increases (pK_a^4 of Quin-2 = 6.25 [Yuchi et al., 1993]), and a resulting spectral change occurs that can be mistaken for Ca^{2+} transport. When these spectral changes are subtracted from Ca^{2+} transport data before they are calibrated, the minor pH dependence seen in Fig. 4 *A* is substantially eliminated (data not shown). Accordingly, alterations in the pH gradient are unlikely to influence the rate of Ca^{2+} transport in the presence of CCCP.

In addition to varying the pH, activation of Ca^{2+} transport afforded by CCCP was determined as a function of the CCCP concentration. When no membrane potential is present initially, the rate is a function of the CCCP concentration (data not shown), even when it exceeds a range required to collapse the inside positive potential created by Ca^{2+} transport based on earlier data (Erdahl et al., 1994, 1995). Furthermore, when an inside negative

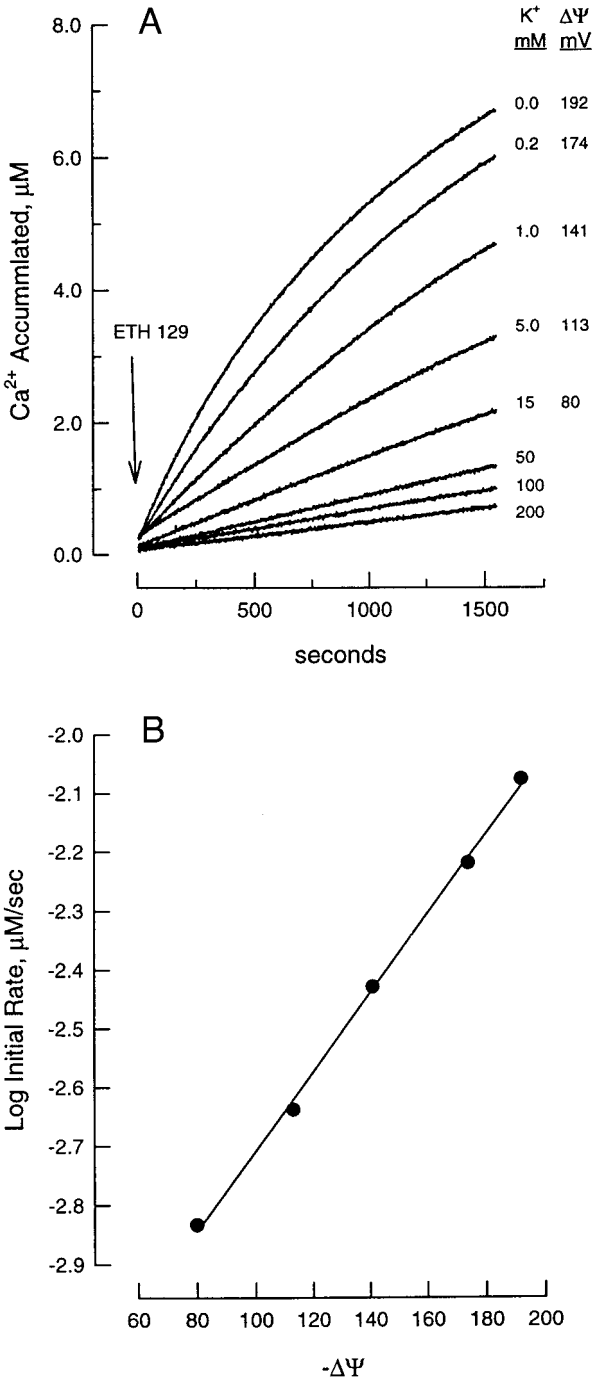

FIGURE 3 Effect of membrane potential on the rate of transport. (*A*) vesicles were incubated as described in Experimental Procedures and the legend to Fig. 2 except the concentrations of POPC and $CaCl_2$ were 1.5 mM and 30 μM, respectively. The external Na^+ concentration was progressively lowered by equimolar replacement with K^+ to reduce the membrane potential formed through the action of Val to desired values (total concentration of $Na^+ + K^+ = 200$ mM). The external K^+ concentrations and observed values of the potential that resulted are shown next to the individual traces. Val was present from the beginning, and transport was initiated by the addition of 5.0 μM ETH-129, as indicated. (*B*) Log initial rate values are shown as a function of the induced potential. Potentials less than ~60 mV cannot be accurately determined under the conditions used.

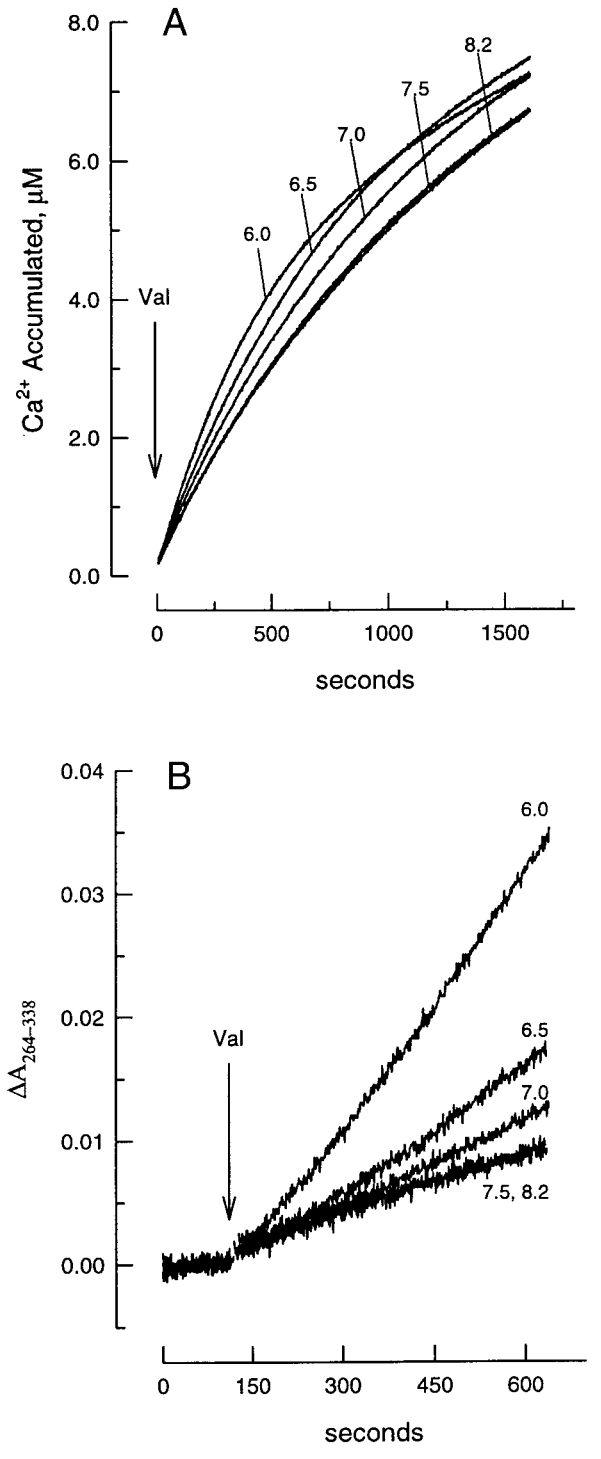

FIGURE 4 Effect of pH conditions on the rate of transport. (*A*) Conditions were the same as described for Fig. 3 *A* except that external Na^+ concentration was 100 mM and K^+ was not added. 5 mM each of Hepes and 2-(*N*-morpholino)ethanesulfonic acid were used instead of Hepes alone, and the pH was varied as indicated. 5.0 μM ETH-129 was present from the beginning with the time of Val addition designated as 0 s. (*B*) Experiments are analogous to those shown in (*A*) except that Ca^{2+} was not present in the medium. The difference absorbance wavelength pair used (*y*-axis) was the same one used for monitoring Ca^{2+} transport. In this case increasing ΔA reflects a more acidic vesicle lumen.

membrane potential is produced and maintained by Val, the rate of Ca^{2+} transport increases progressively as the CCCP concentration rises from 0 to 5 μM (Fig. 5A and B). That is to say, the presence of CCCP favors Ca^{2+} transport by a second mechanism, in addition to collapse of opposing potentials that may arise. As will be further described in the Discussion, we take these findings to indicate that CCCP can associate with the ETH-129:Ca^{2+} complex to form a species of reduced charge that crosses the membrane relatively easily. There is apparently some specificity in this action because oleate (a lipophilic fatty acid anion) is ineffective as a substitute for CCCP (Fig. 5 *B*).

Nature of the transporting species and cation selectivity

To investigate the ionophore:cation stoichiometry of the Ca^{2+}-transporting species, we determined the effect of ETH-129 and Ca^{2+} concentration on the rate of transport. The rate is a function of both parameters, as shown in Figs. 6 *A* and 7 *A*. Plots of log rate versus log ionophore or log Ca^{2+} concentration are straight lines that have slope values of 2.8 and 0.7, respectively (Figs. 6 *B* and 7 *B*). The former value is the same as that reported by Prestipino and coworkers, who used conductance measurements and planar lipid bilayers to characterize ETH-129 as a Ca^{2+} ionophore (Prestipino et al., 1993). It supports a predominate transporting species of stoichiometry 3:1, ionophore:cation, consistent with x-ray crystallography data that show that a complex of this stoichiometry is formed between ETH-129 and Ca^{2+} (Neupert-Laves and Dobler, 1982). The latter value is less than the predicted value of 1.0.

Similar experiments conducted using other cations provided the data shown in Fig. 8 and Table 1. Of interest are the findings obtained with La^{3+} that is transported more efficiently than divalent cations if the comparisons are made at cation concentrations below 1 mM (Fig. 8). Among the divalent cations, the conditional selectivity sequence was $Ca^{2+} > Zn^{2+} \approx Sr^{2+} > Co^{2+} \approx Ni^{2+} \approx Mn^{2+}$. Two groups can be identified within this sequence. Ca^{2+}, Zn^{2+}, and Sr^{2+} are transported at rates that vary substantially with the cation concentration. In contrast, the rates Co^{2+}, Ni^{2+}, and Mn^{2+} transport are relatively independent of cation concentration within the range examined, as is also true for La^{3+} transport (Fig. 8 *B*). As a consequence, the selectivity properties of ETH-129 depend upon the cation concentration range that is considered. Possible reasons for this complex behavior are considered under Discussion.

DISCUSSION

Ionophores that transport Ca^{2+} by an electroneutral mechanism, including A23187, 4-BrA23187, and Ionomycin are

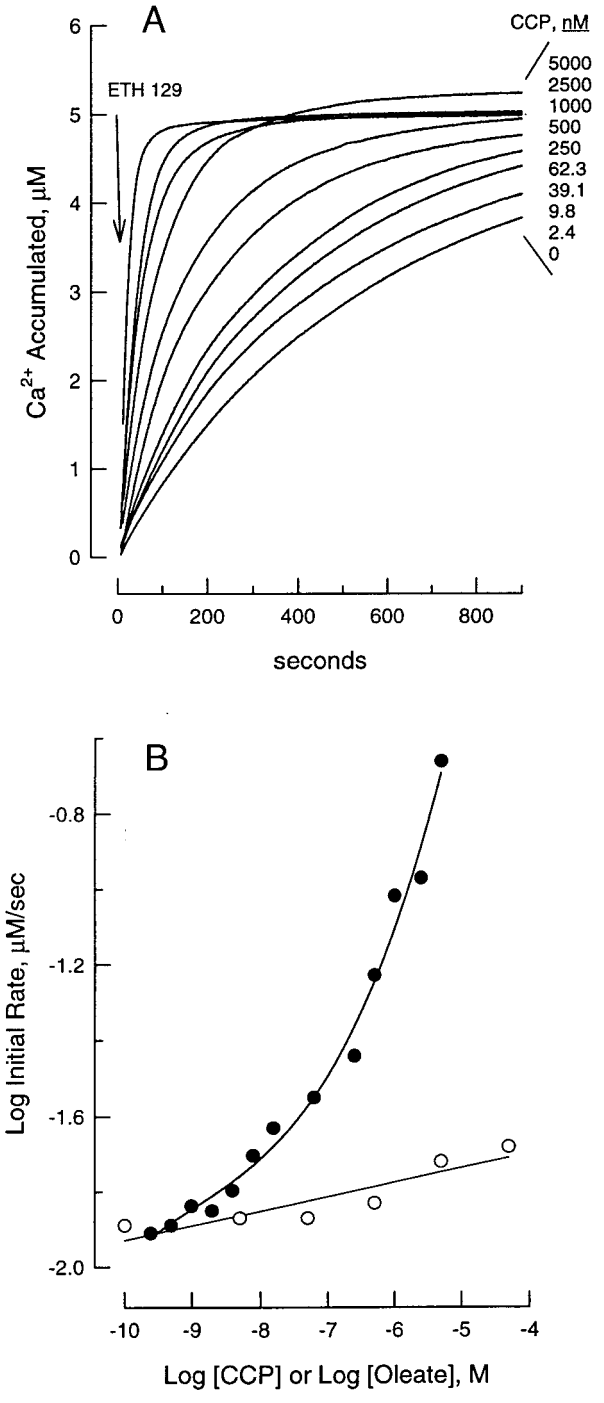

FIGURE 5 Effect of CCCP concentration on the rate of transport. (*A*) Conditions were the same as described for Fig. 3 *A* except that external Na^+ concentration was 100 mM and K^+ was not added. In addition, the concentration of $CaCl_2$ was 1.0 mM and a reduced concentration of Quin-2 had been used when preparing the vesicles (resulting in a reduced content of entrapped Quin-2). Various concentrations of CCCP were present, as indicated in sequence to the right of the individual traces. (*B*) Log initial rate values from (*A*) are expressed as a function of Log CCCP concentration (●). For clarity, some of the traces represented were not shown in (*A*). (○), Values were obtained from a set of experiments like those shown in Panel (*A*), except that various concentrations of oleic acid (18:1) had been used instead of CCCP.

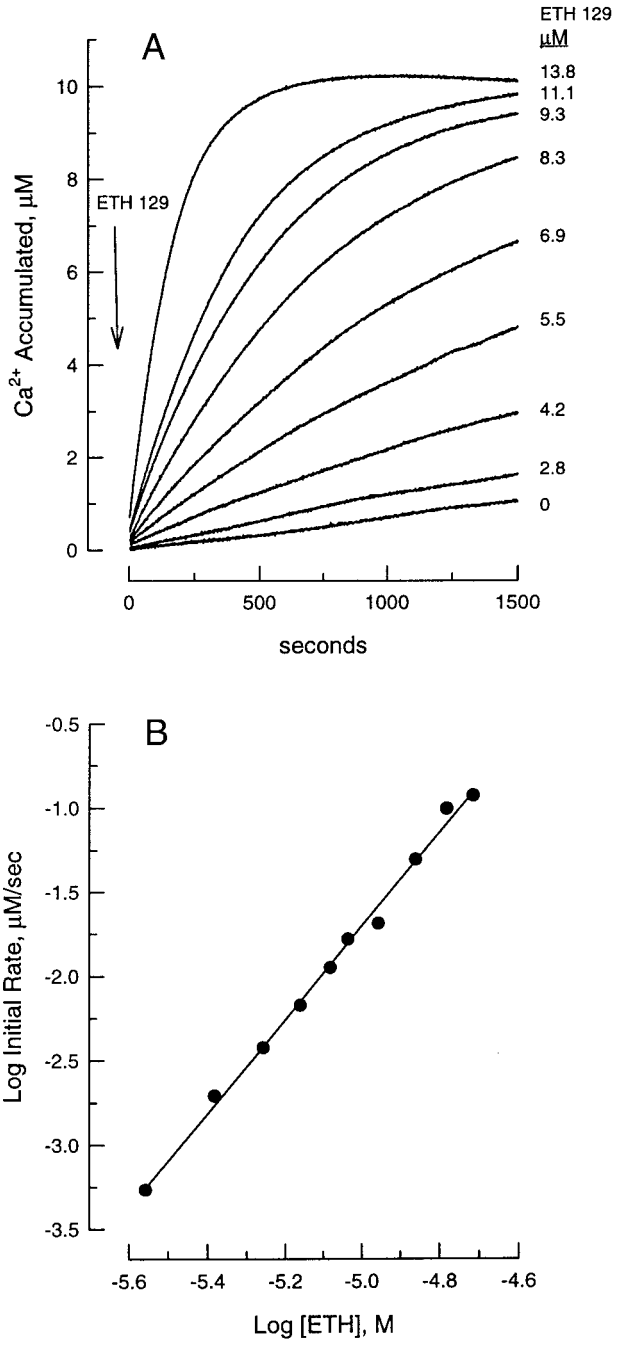

FIGURE 6 Effect of ionophore concentration on the rate of transport. (*A*) Conditions were the same as described for Fig. 3 *A*, except the medium concentration of Na^+ was 100 mM and K^+ was not added. Val was present from the beginning, with transport initiated by the addition of ETH-129 at the indicated concentration. (*B*) Log initial rate values are shown as a function of log ETH-129 concentration.

relatively well-characterized and valuable research tools, but there are no analogous compounds in general use that transport Ca^{2+} electrogenically. This study extends the limited information available on the transport properties of ionophore ETH-129 and shows that this compound is well

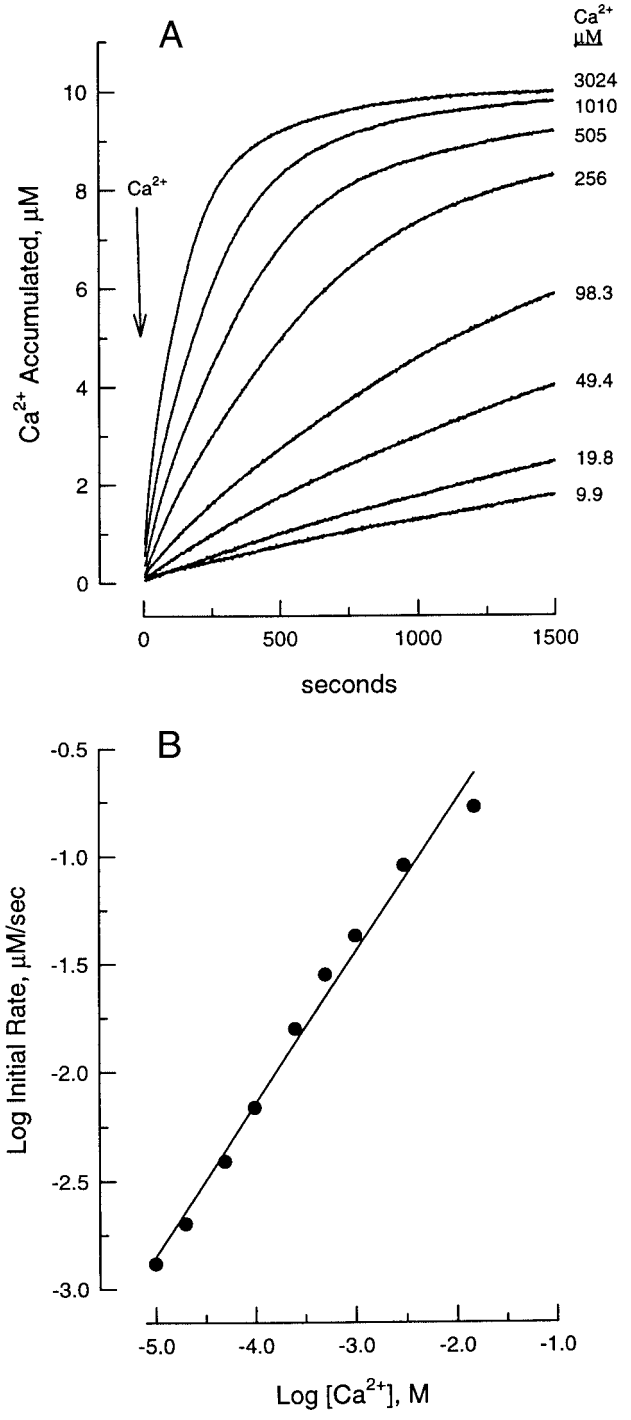

FIGURE 7 Effect of Ca^{2+} concentration on the rate of transport. (*A*) conditions were the same as described for Fig. 5, except the medium Ca^{2+} concentration was varied as shown. ETH-129 (5.0 μM) and Val (0.5 μM) were present from the beginning, with transport initiated by the addition of Ca^{2+} as shown. (*B*) Log initial rate values are shown as a function of log Ca^{2+} concentration.

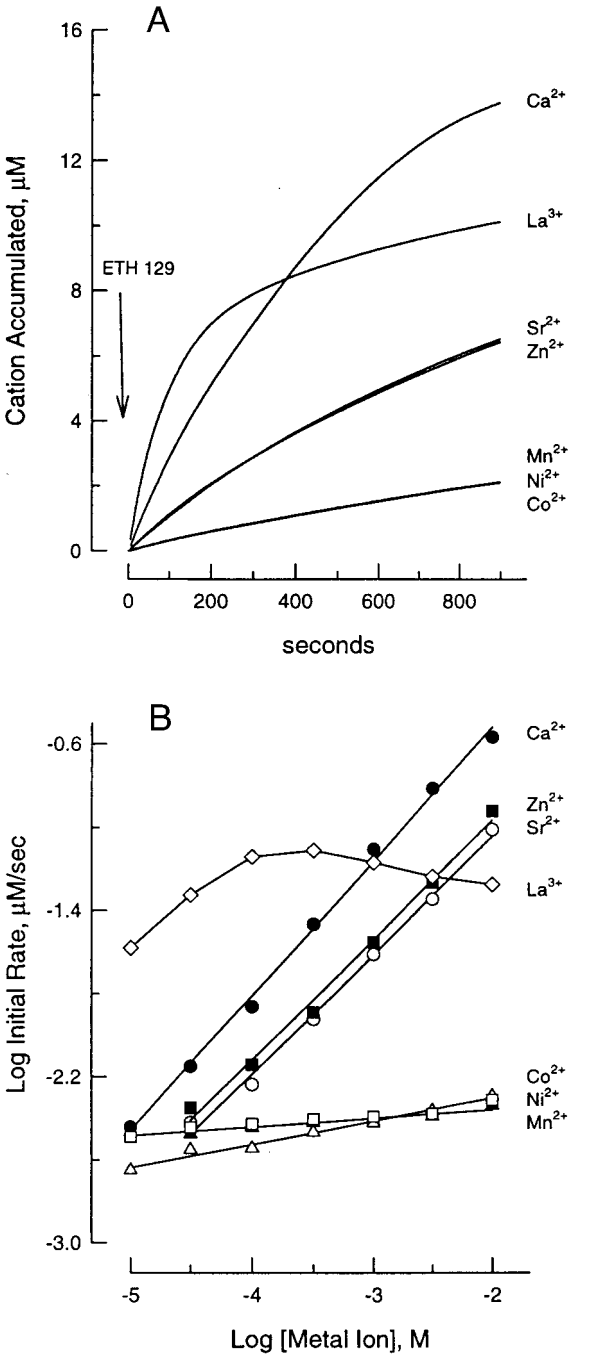

FIGURE 8 Specificity of transport. (*A*) Conditions were the same as described for Fig. 3 *A*, except the medium concentration of Na^+ was 100 mM and K^+ was not added. 30 μM of the indicated cation chloride and Val were present from the beginning. Transport was initiated by the addition of 5 μM ETH-129, as indicated. (*B*) Log initial rate values are shown as a function of log cation concentration. The values were obtained as described for panel A except the cation concentration was varied as shown.

suited for such applications. In particular, we saw no evidence that ETH-129 perturbs the POPC bilayer that limits our vesicles, apart from promoting ion transport. These findings, together with the maintenance of coupled function in mitochondria exposed to similar concentrations of the compound (Prestipino et al., 1993; Jung et al., 1997), indi-

TABLE 1 Concentration dependence and selectivity parameters for the transport of selected cations by ETH 129*

Parameter	Cation						
	Sr^{2+}	Ca^{2+}	Mn^{2+}	Co^{2+}	Ni^{2+}	Zn^{2+}	La^{3+}
$Slope_{ETH-129}$	2.0	1.5	0.85	0.55	0.78	ND	ND
$Slope_{Me}$	0.57	0.65	0.04	0.11	0.05	0.58	nonlin
Selectivity, Ca/Me							
$10^{-2.0}$ M cations	2.8	≡1.0	59	53	55	2.3	5.1
$10^{-3.5}$ M cations	2.9	≡1.0	8.9	9.9	8.6	2.6	0.44
$10^{-5.0}$ M cations	1.0	≡1.0	1.1	1.6	1.1	0.9	0.14

*$Slope_{Me}$ values were obtained from the data shown in Fig. 8 *B*. Selectivity values are from the same data and represent the rate of Ca^{2+} transport divided by the rate for the cation of interest when both cations were present at the indicated concentration. $Slope_{ETH-129}$ values were obtained from experiments like those shown in Fig. 6, except that the cation concentration used was 1.0 mM.

cate that a minimum of nonspecific effects should be encountered in vivo.

Along similar lines, the related compound ETH-1001 was reported to transport Na^+ and K^+ at efficiencies similar to that of Ca^{2+} (Caroni et al., 1977; Vuilleumier et al., 1977). However, during this study, there was no evidence that ETH-129 is significantly active for the transport of either alkali cation. The data in Fig. 2 are pertinent in this regard. If ETH-129 were able to transport K^+ electrogenically at a significant rate, one would expect a rapid rate of Ca^{2+} transport into K^+-loaded vesicles in the presence of that ionophore alone. This is because ETH-129 would promote electrogenic Ca^{2+} entry and electrogenic K^+ release, resulting overall in a neutral exchange of Ca^{2+} for $2K^+$. Instead, it was seen that Ca^{2+} is transported very slowly by ETH-129 alone (Fig. 2 *A*), but rapidly when Val is also present (Fig. 2 *B*). Thus, the neutral exchange of Ca^{2+} for $2K^+$ in this system requires the presence of an authentic electrogenic ionophore for K^+. Regarding Na^+, if ETH-129 were effective as an electrogenic ionophore for Na^+, the membrane potential induced by Val-mediated K^+ release in a Na^+-containing medium (Fig. 2 *B*) would rapidly collapse upon the addition of ETH-129 in the absence of external Ca^{2+}. An experiment of this type showed only a small effect of ETH-129 on membrane potential under those conditions (data not shown). Thus, Na^+ is also transported slowly in comparison to Ca^{2+}.

The extent of selectivity for Ca^{2+} over monovalent cations may, in fact, be substantially higher for ETH-129, compared to ETH-1001. However, the data indicating that ETH-1001 transports K^+ were obtained by investigating mitochondrial swelling due to the entry of K^+ and acetate from an external medium. Since that work was conducted, several mitochondrial activities have been discovered that might have been responsible for the observed swelling, without a direct involvement of K^+ transport mediated by ETH-1001 (Gunter and Pfeiffer, 1990; Sorgato and Moran, 1993; Brierley et al., 1994). Similarly, the phospholipid vesicles used to investigate Na^+ transport were formed by sonication using lipids of unspecified purity. The high surface curvature of small vesicles derived by sonication results in preparations that are less stable than the larger vesicles used here (Nayar et al., 1989). This factor, together with possible perturbation by impurities and the high levels of ETH-1001 that were used, may have contributed to the apparent rates of Na^+ transport. Clearly, additional work will be required to fully evaluate the relative properties of these two ionophores, and to obtain quantitative estimates of their Ca^{2+}/monovalent cation selectivities across a range of conditions. However, the present data do suggest that ETH-129 is more suitable than ETH-1001 for use in biological systems.

ETH-129 is thought to transport Ca^{2+} as the 3:1 complex, ionophore:cation, based on x-ray crystallography data and a transport study that used planar lipid bilayers (Neupert-Laves and Dobler, 1982; Prestipino et al., 1993). The dependence of initial rate on ionophore concentration (Fig. 6) and Ca^{2+} concentration (Fig. 7) are largely consistent with this view. However, the slopes of the log versus log plots in these figures differ from the values of 3.0 and 1.0, respectively, that are expected if the 3:1 complex were the only species that transports Ca^{2+} (the observed slopes were 2.8 and 0.7). In addition, the slope of the log rate versus log ETH-129 concentration plot was decreased to 1.5 when the Ca^{2+} concentration was increased from 100 μM (Fig. 7) to 1.0 mM (Table 1). These findings can be rationalized if more than one species transports Ca^{2+}. More specifically, the 3:1 complex that is thought to be the primary transporting species would be subject to the comproportionation equilibria represented by (charges omitted).

$$(ETH)_3Ca + Ca \leftrightarrows (ETH)_2Ca + ETHCa, \quad (1)$$

$$(ETH)_2Ca + Ca \leftrightarrows 2ETHCa. \quad (2)$$

If the 2:1 or 1:1 complexes were also able to transport Ca^{2+}, the slope of a log rate versus log ionophore concentration plot would be less than 3, in proportion to the prevalence of the various complexes and their relative efficiencies as transporting species. This can explain how a slope of 2.8 might arise under the conditions of Fig. 6. From Eqs. 1 and 2, the prevalence of the 2:1 and 1:1 complexes would increase as the Ca^{2+} concentration increased. This would cause the slope to fall further below the expected value of 3, explaining the value of 1.5 that was seen under the conditions of Table 1. The formation of impermeant complexes containing more than one Ca^{2+} and a probable inefficient transport by the 1:1 complex probably explains the lower than expected slope of the log rate versus log Ca^{2+} concentration plot seen in Fig. 7.

In addition to complexes between ETH-129 and Ca^{2+} alone, it also appears that ETH-129 can transport Ca^{2+} via mixed complexes that include a lipophilic anion. This is indicated by the steep rise in the initial rate of Ca^{2+} transport that is seen as the CCCP concentration is increased (Fig. 5). The concentration dependence does not represent a requirement to fully collapse an opposing potential arising from Ca^{2+} transport because it is seen in K^+-loaded vesicles, suspended in a Na^+-based medium, when Val is present. No opposing potential can arise under these conditions and, in fact, Ca^{2+} transport is already supported by the K^+ electrochemical gradient when CCCP is absent. Data like those in Fig. 5 could arise if CCCP associates with ETH-129:Ca^{2+} complexes to form mixed complexes of reduced charge, that permeate the membrane efficiently relative to the corresponding complex between the ionophore and Ca^{2+} alone. Supporting this view, earlier studies showed that lipophilic cations and anions can interact and thereby cross membranes in a facilitated manner (Ginsburg and Stark, 1976; Stark, 1980). In addition, ETH-1001-mediated Ca^{2+} transport is enhanced by the protonophore FCCP (Vuilleumier et al., 1977), and the thiocyanate anion was found to associate with the $(ETH)_3Ca^{2+}$ complex by x-ray crystallography (Neupert-Laves and Dobler, 1982). It is then interesting to observe that the free fatty acid oleate is not effective at enhancing the rate of ETH-129-mediated transport (Fig. 5). Protonophores effectively delocalize net charge through inductive/resonance effects, whereas this is not true for fatty acids. Accordingly, charge delocalization and steric factors may explain why CCCP is more effective than the fatty acid.

Unlike monovalent cations, ETH-129 is quite active as an ionophore for the trivalent La^{3+}, and actually transports that cation more efficiently than Ca^{2+} at concentrations below 1 mM (Fig. 8). This is similar to the electroneutral Ca^{2+} ionophores that transport La^{3+} as effectively as Ca^{2+} under some conditions (Wang et al., 1998). With ETH-129, the predominate transporting species may be $[(ETH)_3LaOH]^{2+}$ because that species would effectively shield the cation from solvation by H_2O, whereas the hydroxide anion would limit net positive charge to the same value that occurs in the predominate species that transports Ca^{2+}. This is also analogous to the situation with electroneutral Ca^{2+} ionophores where mixed complexes that include OH^- allow these compounds to transport trivalent cations via neutral mechanisms based on 2:1 complexes (ionophore:cation) (Wang et al., 1998).

Many of the factors already considered are probably involved in establishing the selectivity patterns illustrated in Fig. 8. For example, the comproportionation equilibria involving Co^{2+}, Ni^{2+}, and Mn^{2+} are apparently shifted to the right, in comparison to those involving Ca^{2+} and Sr^{2+}, based upon the lower slope values obtained from plots of log rate versus log ETH-129 concentration (Table 1). If the 2:1 and 1:1 complexes that are formed with these cations were relatively impermeant, compared to the 3:1 complex, this factor could explain why the former group is transported relatively slowly and with a minimal dependence on cation concentration over the range examined. A differing tendency of these cations to associate with the membrane surface, where the transporting species are formed, may also be a factor in establishing the selectivity sequence observed.

Missing from the group of cations considered is Mg^{2+}, which is present in biological systems at a much higher concentration than the other examples. Mg^{2+} transport cannot be readily investigated with the present vesicle system because it is bound with low affinity by Quin-2 (Yuchi et al., 1993). To obtain some indication of the potential for interference by Mg^{2+} with Ca^{2+} transport in vivo, we determined whether 1.0 mM external Mg^{2+} could facilitate the slow release of Ca^{2+} from Ca^{2+}-loaded vesicles treated with ETH-129. Little effect was seen (data not shown), suggesting that the potential produced by ETH-129-mediated Ca^{2+} release was not cancelled by the electrogenic transport of Mg^{2+} in the opposite direction. This apparent minimal activity as a Mg^{2+} ionophore is a further characteristic supporting the potential of this compound for use as an electrogenic Ca^{2+} ionophore in biological systems.

Given the strong dependence of ETH-129-mediated Ca^{2+} transport on membrane potential (Fig. 3) one expects that the mitochondria in cells treated with this compound would become loaded with high levels of Ca^{2+}. This is because of the inside negative membrane potential that exists in mitochondria and its very large magnitude in comparison to the potentials across other cellular membranes. In mammalian cells, where mitochondria contain the electrogenic Ca^{2+} uniporter, the ionophore would act directly at the inner mitochondrial membrane, but should also enhance Ca^{2+} accumulation via the uniporter. The latter action is expected because ETH-129 would increase the cytoplasmic Ca^{2+} concentration by transporting Ca^{2+} into the cell in response to the small inside negative potential across the plasma membrane. Thus, ETH-129 should prove useful for investigating the consequences of mitochondrial Ca^{2+} overloads in vivo, which presumably include excessive activity of the TCA cycle and occurrence of the permeably transition.

This research was supported by The Wallace Research Foundation, by a grant from the American Heart Association (Award Number 0050992B0), and by MitoKor Inc., San Diego, CA.

REFERENCES

Ammann, D., R. Bissig, Z. Cimerman, U. Fiedler, M. Güggi, W. E. Morf, M. Oehme, H. Osswald, E. Pretsch, and W. Simon. 1976. *In* Ion and Enzyme Electrodes in Biology and Medicine. M. Kessler, L. C. Clark, Jr., D. W. Lübbers, I. A. Silver, and W. Simon, editors. chap. 1. Urban and Schwarzenberg, Muchen, Germany. 22–37.

Bartlett, G. R. 1959. Phosphorous assay in column chromatography. *J. Biol. Chem.* 234:466–468.

Brierley, G. P., K. Baysal, and D. W. Jung. 1994. Cation transport systems in mitochondria: Na^+ and K^+ uniports and exchangers. *J. Bioenerg. Biomembr.* 26:519–526.

Broekemeier, K. M., C. K. Klocek, and D. R. Pfeiffer. 1998. Proton selective form of the mitochondrial permeability transition pore; regulation by the redox state of the electron transport chain. *Biochemistry.* 37:13059–13065.

Caroni, P., P. Gazzotti, P. Vuilleumier, W. Simon, and E. Carafoli. 1977. Ca^{2+} transport mediated by a synthetic neutral Ca^{2+}-ionophore in biological membranes. *Biochim. Biophys. Acta.* 470:437–445.

Chapman, C. J., W. L. Erdahl, R. W. Taylor, and D. R. Pfeiffer. 1990. Factors affecting solute entrapment in POPC vesicles prepared by the freeze-thaw extrusion method. *Chem. Phys. Lipids.* 55:73–83.

Chapman, C. J., W. L. Erdahl, R. W. Taylor, and D. R. Pfeiffer. 1991. Effect of solute concentration on the entrapment of solutes in phospholipid vesicles prepared by freeze–thaw extrusion. *Chem. Phys. Lipids.* 60:201–208.

Dobler, M. 1981. Classification of ionophores. *In* Ionophores and Their Structures. John Wiley and Sons, New York.

Erdahl, W. L., C. J. Chapman, R. W. Taylor, and D. R. Pfeiffer. 1994. Ca^{2+} transport properties of ionophores A23187, ionomycin, and 4-BrA23187 in a well defined system. *Biophys. J.* 66:1678–1693.

Erdahl, W. L., C. J. Chapman, R. W. Taylor, and D. R. Pfeiffer. 1995. Effects of pH conditions on Ca^{2+} transport catalyzed by ionophores A23187, 4-BrA23187, and ionomycin suggest problems with common applications of these compounds in biological systems. *Biophys. J.* 69: 2350–2363.

Erdahl, W. L., C. J. Chapman, R. W. Taylor, and D. R. Pfeiffer. 2000. Ionomycin, a carboxylic acid ionophore, transports Pb^{2+} with high selectivity. *J. Biol. Chem.* 275:7071–7079.

Erdahl, W. L., C. J. Chapman, E. Wang, R. W. Taylor, and D. R. Pfeiffer. 1996. Ionophore 4-BrA23187 transports Zn^{2+} and Mn^{2+} with high selectivity over Ca^{2+}. *Biochemistry.* 35:13817–13825.

Fry, D. W., J. C. White, and D. Goldman. 1978. Rapid separation of low molecular weight solutes from liposomes without dilution. *Anal. Biochem.* 90:809–815.

Ginsburg, H., and G. Stark. 1976. Facilitated transport of di- and trinitrophenolate ions across lipid membranes by valinomycin and nonactin. *Biochim. Biophys. Acta.* 455:685–700.

Gunter, T. E., and D. R. Pfeiffer. 1990. The mechanisms by which mitochondria transport calcium. *Am. J. Physiol. Cell Physiol.* 258: C755–C786.

Jung, D. W., P. C. Bradshaw, and D. R. Pfeiffer. 1997. Properties of a cyclosporin-insensitive permeability transition pore in yeast mitochondria. *J. Biol. Chem.* 272:21104–21112.

Nayar, R., M. J. Hope, and P. R. Cullis. 1989. Generation of large unilamellar vesicles from long-chained saturated phosphatidylcholines by extrusion technique. *Biochim. Biophys. Acta.* 986:200–206.

Neupert-Laves, K., and M. J. Dobler. 1982. Crystal structure analysis of divalent metal cation complexes with neutral noncyclic ionophores. II. Mg^{2+} and Ca^{2+} complexes of *N*,*N*,*N*′,*N*′-tetracyclohexyl-3-oxapentanediamide. *Crystallogr. Spectrosc. Res.* 12:287–299.

Prabhananda, B. S., and M. H. Kombrabail. 1998. Evidence for dimer participation and evidence against channel mechanism in A23187-mediated monovalent metal ion transport across phospholipid vesicular membrane. *Biophys. J.* 75:1749–1758.

Prestipino, G., C. Falugi, R. Falchetto, and P. Gazzotti. 1993. The ionophore ETH-129 as Ca^{2+} translocator in artificial and natural membranes. *Anal. Biochem.* 210:119–122.

Pretsch, E., D. Ammann, H. Osswald, M. Güggi, and W. Simon. 1980. Ionophore vom typ der 3-oxapentandiamide. *Helv. Chim. Acta.* 63: 191–196.

Schefer, U., D. Ammann, E. Pretsch, U. Oesch, and W. Simon. 1986. Neutral carrier based Ca^{2+}-selective electrode with detection limit in the sub-nanomolar range. *Anal. Chem.* 58:2282–2285.

Sorgato, M. C., and O. Moran. 1993. Channels in mitochondrial membranes: knowns, unknowns, and prospects for the future. *Crit. Rev. Biochem. Mol. Biol.* 28:127–171.

Stark, G. 1980. Negative hydrophobic ions as transport-mediators for positive ions. *Biochim. Biophys. Acta.* 600:233–237.

Thomas, T. P., E. Wang, D. R. Pfeiffer, and R. W. Taylor. 1997. Evidence against formation of A23187 dimers and oligomers in solution: photoinduced degradation of ionophore A23187. *Arch. Biochem. Biophys.* 342:351–361.

Vuilleumier, P., P. Gazzotti, E. Carafoli, and W. Simon. 1977. The translocation of Ca^{2+} across phospholipid bilayers induced by a synthetic neutral Ca^{2+}-ionophore. *Biochim. Biophys. Acta.* 467:12–18.

Wang, E., R. W. Taylor, and D. R. Pfeiffer. 1998. Mechanism and specificity of lanthanide series cation transport by ionophores A23187, 4-BrA23187, and ionomycin. *Biophys. J.* 75:1244–1254.

Westley, J. W. 1982. Notation and classification. *In* Polyether Antibiotics: Naturally Occurring Acid Ionophores. J. W. Westley, editor. Marcel Dekker, New York.1–20.

Woolley, G. A., D. R. Pfeiffer, and C. M. Deber. 1995. The use of ionophores for manipulating intracellular ion concentrations. *In* Methods in Neurosciences. J. Krajcer and S. J. Dixon, editors. Academic Press, Orlando, FL. 52–68.

Yuchi, A., A. Tanaka, M. Hirai, T. Yasui, H. Wada, and G. Nakagawa. 1993. Complexation equilibria and fluorescent properties of chelating reagents derived from ethylene glycol bis (β-aminoethylether)-*N*,*N*,*N*′,*N*′-tetraacetic acid. *Bull. Chem. Soc. Jpn.* 66:3377–3381.